Influence of Entanglements on the Viscoelastic Relaxation of Polyurethane Melts and Gels

Ekatarina Gasilova,† Lazhar Benyahia, Dominique Durand, and Taco Nicolai*

Polymères, Colloïdes, Interfaces, UMR CNRS, Université du Maine, 72085 Le Mans Cedex 9, France

Received August 6, 2001

ABSTRACT: The frequency dependence of the shear modulus was studied for cross-linked polyurethane melts and gels at various cross-link densities. The polyurethane used in this study was based on mixtures of bifunctional linear poly(propylene oxide) (PPO) and trifunctional star PPO end-linked with diisocyanate. The connectivity extent was varied by varying the stoichiometric ratio of hydroxyl groups and isocyanate groups. The results were compared with mean field theory predictions. Relaxation of trapped entanglements was observed for almost fully end-linked systems containing a very low concentration of trifunctional PPO.

Introduction

Cross-linking flexible polymers leads to the formation of randomly branched polymers. With increasing connectivity extent, p, the polymer aggregates grow in size until a system spanning network is formed at a critical value, p_c. As the connectivity extent is further increased, more and more aggregates attach to the gel, which reduces the sol fraction. The sol−gel transition is characterized by the divergence of the viscosity and the appearance of an elastic modulus. The gelation process has been studied experimentally for many systems and two theoretical approaches have been used predominantly to interpret the experimental results.

The first approach is a mean field theory introduced by Flory and Stockmayer.[1,2] In this approach, excluded volume interaction and (large-scale) cyclization are ignored and the reactivity of a particular site is supposed to be independent of its position. By use of mean field theory, p_c can be calculated from system composition and the functionality of the cross-links. In addition, parameters such as the gel fraction (w_{gel}) and the number of elastically active chains can be calculated analytically. The main problem with this theory, however, is that it predicts that the density of the aggregates will increase linearly with their radius. Clearly, mean field theory fails close to the gel point where the radius of the aggregates diverges.

The second approach is the percolation model,[3] which accounts for excluded volume interaction and cyclization. Unfortunately, the percolation model cannot be solved analytically, but large-scale properties of the aggregates and the gel have been obtained by numerical simulations. Properties that depend on the local structure of a particular system cannot be addressed by this model. For instance, Monte Carlo simulations have shown how close to the gel point the weight-average molar mass (M_w) of the aggregates and w_{gel} scale with $\epsilon = |p - p_c|/p_c$, but the prefactors of these scaling relations and the value of p_c are not related to those of real systems.

Over the last two decades much attention has been focused on establishing whether the percolation model is appropriate to describe the sol−gel transition of real systems. Accumulated evidence appears to support the percolation model, but we stress that this model can only describe the system at length scales much larger than that between branching points. Such very large clusters are only formed in a very narrow region of p close to p_c. On the other hand, the assumptions of mean field theory are only reasonable for clusters with low aggregation numbers. Over a range of intermediate p-values, neither model is appropriate. A complete description of the gelation process demands more realistic numerical simulations that are as yet not possible.

Mean field theory and the percolation model describe the structural properties of the cross-linked system and form the basis for the interpretation of the viscoelastic properties. Up till the gel point the viscoelastic relaxation is due to conformational relaxation of the aggregates. The relaxation on large length scales, i.e., much larger than the size of the precursors, has been described in terms of a series of normal modes using the percolation model for the fractal structure of the aggregates and their power law size distribution.[4,5] It is furthermore assumed that hydrodynamic interactions are screened by small aggregates that interpenetrate larger aggregates. The result of this calculation is that the storage and loss shear modulus have a power law dependence on the frequency ($G' \propto G'' \propto \omega^{\Delta}$), with the exponent $\Delta = 0.7$. This behavior has indeed been observed experimentally for various systems based on small precursors very close to the gel point. However, if large precursors are used this behavior cannot be observed experimentally, because the relevant relaxation times are too long.

It is generally assumed that the gel is formed first by the largest aggregates and that smaller and smaller aggregates attach to the gel with increasing connectivity extent. The size of the largest aggregates of the sol has the same order of magnitude as the distance between cross-links (R^*). If the system is homogeneous at length

* Corresponding author.
† Permanent address: Institute of Macromolecular Compounds, St. Petersburg, Russia.

10.1021/ma011412a CCC: $22.00
Published on Web 12/06/2001

scales larger than R^*, then the response to mechanical deformation on these larger length scales will be purely elastic and characterized by an elastic modulus G_0. G_0 has been related to the number concentration of elastically active chains (ν) as[6] $G_0 = a\nu kT$, where a is a prefactor that depends on the assumptions of the model. In the limiting case of affinely deforming networks $a = 1$, while for freely moving cross-links a depends on the functionality of the cross-links (f): $a = 1 - (2/f)$. The viscoelastic relaxation after the gel point is the sum of that of the gel fraction and that of the sol fraction. The viscoelastic relaxation of the gel fraction on length scales smaller than R^* can be calculated in the same way as for the sol fraction because the structure is the same as that of the aggregates. The difference is that the extreme polydispersity of the sol fraction modifies the value of Δ, whereas the chain fragments between cross-links are not so polydisperse. As a consequence the gel fraction leads to a power law frequency dependence of the shear modulus with a smaller exponent. At frequencies below that where the normal modes with size R^* relax, G' is expected to be independent of ω, while $G'' \propto \omega$.

In the foregoing discussion it has been assumed that topological interactions, i.e., entanglements, play no role. However, in covalently cross-linked gels, entanglements may become permanently trapped and thereby contribute to G_0 if the average molar mass between cross-links (M_c) is larger than the average molar mass between entanglements (M_e). Molecular dynamics simulations[7] and experiments[8] on end-linked linear chains showed that about two trapped entanglements have the same contribution as one permanent cross-link. Few studies have addressed the influence of entanglements on the frequency dependence of the shear modulus at different connectivity extents. Recently, we showed that even if the precursors are weakly entangled then the relaxation of the shear modulus is dramatically slowed compared to that of unentangled precursors at the same connectivity extent.[9] The aim of the present study was to investigate the influence of entanglements on the gelation process over the whole range of connectivity extents.

It is difficult to cross-link highly entangled precursors in a controlled way, because such systems are very viscous. Therefore we used a different approach in which we introduced the entanglements during the gelation process of unentangled precursors. Generally, cross-linking of unentangled precursors does not lead to the formation of entanglements because the aggregates have a branched structure. An exception is the case where the precursors are end-linked by both bifunctional and multifunctional linking agents. If purely bifunctional linking agents are used then a system of long entangled chains is formed, whereas if purely multifunctional agents are used then only covalent cross-links are formed. One can vary the fraction of entanglements by varying the ratio between the number of bifunctional and multifunctional linking agents. If one chooses the molar mass of the precursor to be close to that between entanglements, then at complete reaction, each bifunctional linking agent leads to an entanglement and each multifunctional agent leads to a covalent cross-link. In this way it should be possible to investigate the difference between the influence of an entanglement and a covalent cross-link on the viscoelastic properties.

In this paper we present an investigation of the viscoelastic relaxation of polyurethane based on mixtures of linear and three-armed star poly(propylene oxide) (PPO) that were end-linked with a diisocyanate. As we will show below, the reactivity of each end group of these polymers is the same. The molar mass of the linear PPO was 4.0 kg/mol, which is close to the entanglement molar mass of PPO, while the molar mass of the star PPO was much smaller (0.72 kg/mol). The resulting system consists of randomly cross-linked entangled chains in which the ratio between entanglements and cross-links is given by the ratio between linear and star PPO. We have investigated the influence of entanglements on the viscoelastic properties by varying this ratio.

Experimental Section

Polyurethanes were formed by polycondensation of poly(oxypropylene) triols and diols with hexamethylene diisocyanate (HMDI) (Aldrich). The PPO triol (T720) and diol (D4000) used in this study have been characterized by size-exclusion chromatography (SEC) with both refractive index and UV absorption detection. The combination of these two detection techniques allows determination of the size distribution and the number of hydroxyl groups per polymer. The number-averaged molar mass (M_n) and polydispersity index (M_w/M_n) are 0.72 kg/mol and 1.02 for T720 and 4.0 kg/mol and 1.05 for D4000, respectively. T720 was fully functionalized whereas D4000 contained a fraction (±5%) of monofunctional material with lower molar mass. We note that the polydispersity indices are overestimated due to intrinsic dispersion effects in the SEC columns.

Systems with different connectivity extents were prepared by varying the ratio of isocyanate groups to hydroxyl groups. Dibutyl tin dilaurate catalyst (2×10^{-3} g) was added for every gram of HMDI. After mixing and complete homogenization of the reaction components, the samples were cured overnight at 40 °C.

Dynamic shear measurements were done on a Rheometrics RDA II dynamic spectrometer with parallel-plate geometry at temperatures between −60 and 100 °C. In the so-called hold mode, the gap is corrected for temperature variations of the sample volume. The plate size (diameter between 50 and 4 mm) and the imposed deformation (0.2−20%) were adjusted to obtain an accurate torque response while remaining in the linear regime.

The gel fraction was determined by measuring the concentration of the sol for highly diluted systems by SEC.

Results

We have prepared a large number of samples with different connectivity extents and different cross-link densities. Different cross-link densities were obtained by varying the molar fraction of triol: $\varphi = n_{B3}/(n_{B3} + n_{B2})$. Different connectivity extents were obtained by varying the molar ratio between the isocyanate groups of HMDI and the hydroxyl groups of PPO: $r = 2n_A/(3n_{B3} + 2n_{B2})$. n_A, n_{B2}, and n_{B3} are the molar concentrations of HMDI, PPO diol, and PPO triol, respectively. For each sample we established whether it contained an insoluble gel fraction by adding a large amount of solvent. In Figure 1 we compare the experimental results with the sol−gel state diagram predicted by mean field theory (see Appendix). The samples indicated by filled circles in Figure 1 were found to be very close to the gel point in the mechanical measurements; see below. We assumed in the calculation complete reaction of the isocyanate groups and we ignored the small fraction of monofunctional linear PPO. There is a good agreement

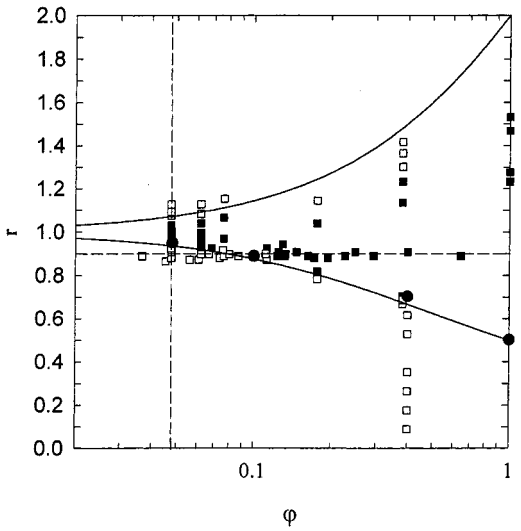

Figure 1. Sol−gel diagram of polyurethane formed by cross-linking linear and star PPO with HMDI. Filled squares represent systems with a measurable gel fraction. Filled circles represent systems with a viscoelastic relaxation typical for systems at the gel point. Unfilled squares represent systems without a discernible gel fraction. The solid lines represent the mean field prediction. The vertical and horizontal dashed lines indicate the position of the data for which the dynamic mechanical spectra are shown in Figures 6 and 7, respectively.

between the experimental results and the prediction from mean field theory for $r < 1$ if we choose for r values that are 12% smaller than the ratios calculated from the weight fractions of PPO and HMDI. For $r > 1$ the agreement is not so good at larger φ, but for a large excess of isocyanate it is difficult to avoid side reactions.

Several reasons may be invoked to explain why we need to use a smaller value of r than that based on the weight fraction: impurity of HMDI, incomplete reaction, formation of loops, and side reactions. Including the small fraction of monofunctional linear PPO in the calculation does not modify the result significantly. We checked by NMR that the purity of HMDI was better than 95%. Furthermore we checked whether the reaction was completed by measuring the shear modulus as a function of time. Figure 2 shows for a number of samples the evolution at 40 °C of G' at $\omega = 1$ rad/s. For almost all samples investigated the reaction is completed after curing overnight at 40 °C. In two cases ($r = 0.98$ and 1.01 at $\varphi = 0.048$) where highly entangled gels were formed we observed a weak continuing growth of G' after this time. All samples close to the gel point that are relevant for the sol−gel diagram had fully reacted. Notice that the fact that we form a gel at all for $\varphi = 0.048$ implies that the reaction extent is at least 0.96; see Appendix. Importantly, loop formation and incomplete reaction would still lead to a phase diagram that is symmetric around $r = 1$. We conclude that a small fraction of the isocyanate has not been used efficiently to form cross-links. The effect of side reactions is more obvious when an excess of isocyanate is used.

In Figure 3 the residual sol fraction of gelled samples is plotted as a function of φ for samples with $r = 0.90 \pm 0.01$, together with the prediction of mean field theory (see Appendix). Again the experimental results are, with one exception, compatible with mean field theory if we use a value of r that is 12% smaller than the value based on the weight fractions of PPO and HMDI.

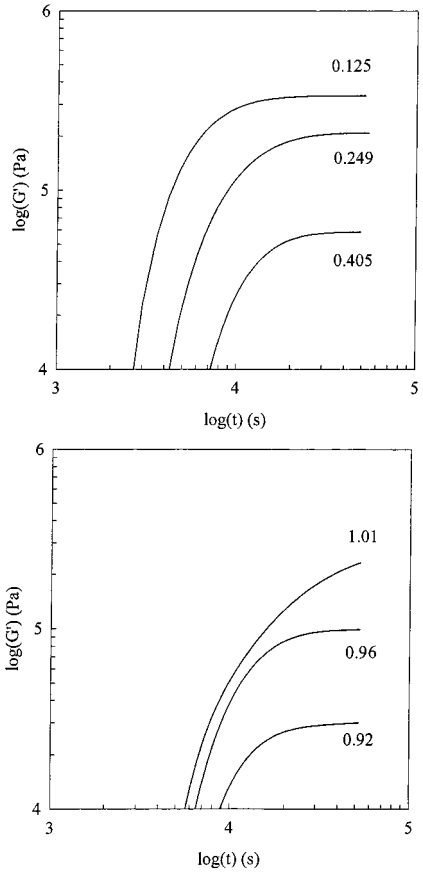

Figure 2. Evolution at 40 °C of the storage shear modulus for systems at $r = 0.9$ and three values of φ (top) indicated in the figure and at $\varphi = 0.048$ and three values of r (bottom).

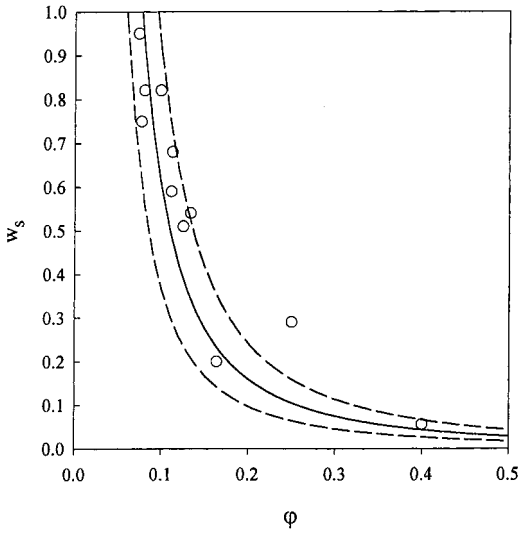

Figure 3. Dependence of the sol fraction at $r = 0.9 \pm 0.01$ as a function of φ. The solid line represents the mean field prediction with $r = 0.90$, while the dashed lines show the predictions with $r = 0.89$ and $r = 0.91$.

Figure 4 shows chromatograms of the system with $\varphi = 0.46$ at various connectivity extents. We have determined the residual weight fraction of monomeric star PPO and monomeric and dimeric linear PPO from the relative peak areas; see ref 10 for details of the procedure. The results are compared with the predictions from mean field theory in Figure 5. For the calculation of the fractions of monomeric and dimeric linear PPO we included all species that contain one or

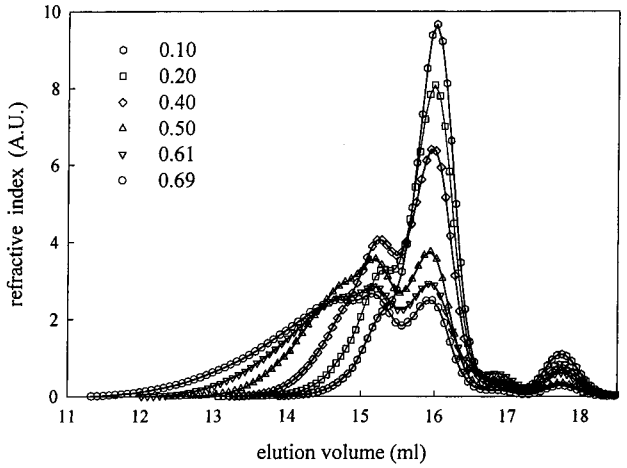

Figure 4. Chromatograms of polyurethane formed at $\varphi = 0.40$ and different values of r indicated in the figure.

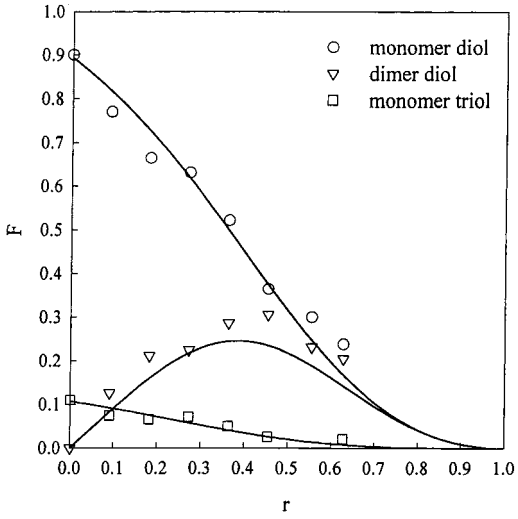

Figure 5. Weight fractions of monomers and dimers of linear PPO and monomers of star PPO. The solid lines represent mean field predictions.

two PPO diols regardless of how many PPO triols they contain. Obviously, if these fractions contain many PPO triols their contribution to the molar mass can no longer be neglected. However, at the value of φ used in the experiment the probability of more than one star PPO per linear PPO is very low. The experimental results for the monomer fractions are in good agreement with the theory, which means that the reactivity of all hydroxyl end groups is the same. The experimental fraction of dimers is somewhat larger than the theory predicts, but it is possible that the difference is caused by the difficulty of separating dimers from larger aggregates in the chromatograms.

We have studied the viscoelastic relaxation of the system both as a function of r at $\varphi = 0.046$ and as a function of φ at $r = 0.9$; see dashed lines in Figure 1. The frequency dependencies of the loss and storage shear moduli were measured over a range of temperatures. Master curves were obtained by time−temperature superposition. It is well established that the local segmental relaxation at high frequencies has a different temperature dependence than the conformational relaxation at lower frequencies,[11] which means that time−temperature superposition is not possible over the whole frequency domain with the same shift factors. However,

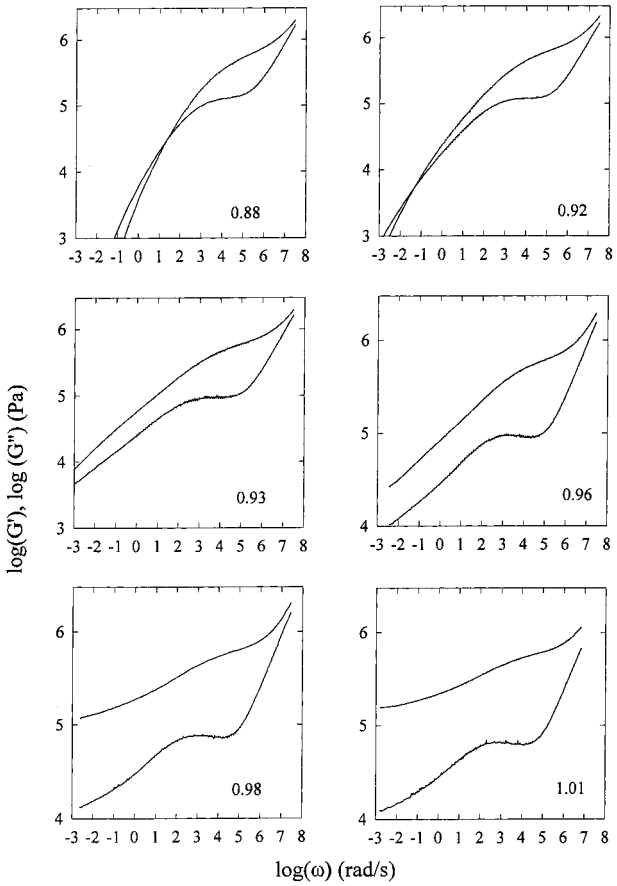

Figure 6. Double logarithmic representation of the frequency dependence of G' and G'' at $\varphi = 0.048$ and different values of r indicated in the figure. $G' > G''$ except in two cases where they cross at a low frequency.

in this paper we show only the conformational relaxation, because the segmental relaxation is not significantly modified by cross-linking the systems studied here. The temperature dependence of the shift factors is the same for all samples after correction for small differences in the glass transition temperature, i.e., if the reference temperature is at the same distance from T_g. It is the same as for linear and star PPO discussed in ref 11.

Figure 6 shows the frequency dependence of G' and G'' at $\varphi = 0.048$ and different values of r close to $r = 1$ (for $r < 0.88$ the relaxation spectrum is similar to that of a melt of linear chains). Figure 7 shows the results at $r = 0.90 \pm 0.01$ at different values of φ. The reference temperature of all master curves is 50 °C. At the highest frequencies one observes the decay of the Rouse modes between entanglements, which leads to $G'' \propto G' \propto \omega^{0.5}$. This power law frequency dependence is clearly observed for G'' but is obscured for G' by the crossover to a very weak frequency dependence that characterizes the relaxation of entanglements. For G'' the crossover is characterized by a minimum at ω_R between 10^4 and 10^5 Hz. Once all the Rouse modes between entanglements have relaxed, the storage modulus is given by the entanglement concentration: $G_e' = RT\rho/M_e$, where R is the gas constant and ρ is the density of the system. For the present system M_e was estimated as 4.0 kg·mol^{-1} by comparing the viscoelastic relaxation of end-linked linear PPO with that of end-linked star PPO, see ref 12. Taking for the density of PPO $\rho = 10^3$ kg·m^{-3}, we find that $G_e' = 6 \times 10^5$ Pa, which is compatible with

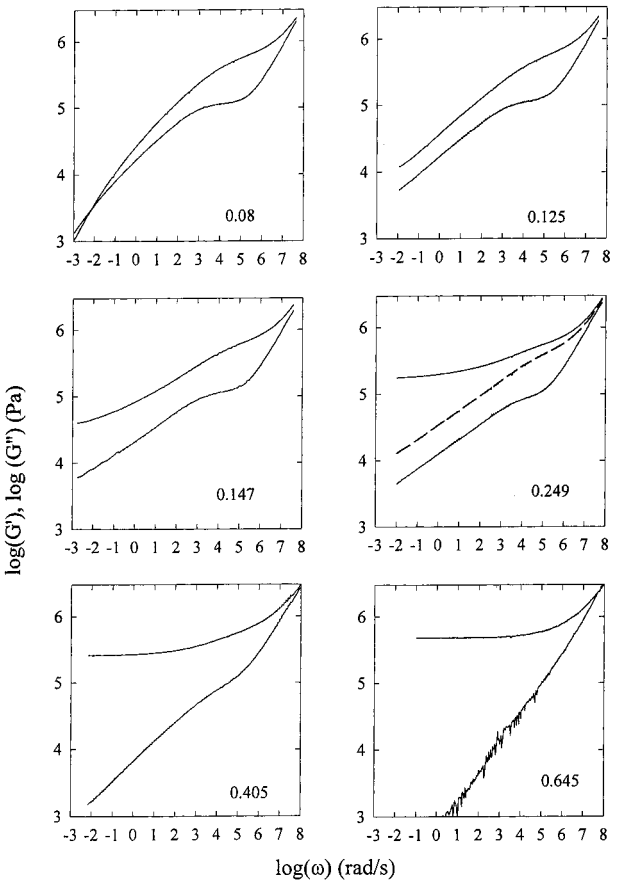

Figure 7. Double logarithmic representation of the frequency dependence of G' and G'' at $r = 0.90$ and different values of φ indicated in the figure. $G' > G''$ except in one case where they cross at a low frequency. The dashed curve in one of the panels represents $G' - G_0$.

the value of G' at ω_R. Of course, the crossover between the conformational relaxation between entanglements and the disentanglement process is not sharp because M_e is only the average of a distribution of molar masses between entanglements.

The high frequency dependence of the shear modulus is the same for all samples as long as the cross-link density is lower than the entanglement density, i.e., as long as $M_c > M_e$. M_c decreases with increasing φ (see Appendix) and equals M_e at $\varphi = 0.4$ for r close to unity. The relaxation of the disentanglement process is characterized by a shoulder or a weak maximum in G''. The position of the shoulder and the maximum may be related to the mean length of linear chains in the system; see below. At larger values of φ the system is no longer entangled and the normal modes relaxation at high frequencies crosses over to the relaxation of branched polymers and the gel.

With increasing r at a fixed value of φ (see Figure 6), larger branched polymers are formed until at a critical value, r_c, the system percolates and a gel is formed. The sol−gel transition is characterized by a divergence of the terminal relaxation time and the appearance of an elastic gel modulus (G_0). The value of r_c increases with decreasing cross-link density and is approximately 0.95 for $\varphi = 0.048$; see Figure 1. Close to the gel point G' and G'' have a power law frequency dependence at low frequencies.

Table 1. Experimental Values of the Power Law Exponent, Δ, and the Elastic Modulus of Gels at Different Values of φ and r[a]

j	r	Δ	G^0 (Pa) exp	G_0 (Pa) theor
0.645	0.89	0.42	7.7×10^5	7.1×10^5
0.400	0.91	0.3	2.7×10^5	2.8×10^5
0.249	0.91	0.22	1.8×10^5	9.8×10^4
0.164	0.89	0.19	4.8×10^4	1.7×10^4
0.147	0.91	0.20	2.1×10^4	2.0×10^4
0.048	0.98	0.12	6.4×10^4	7.2×10^3
0.048	1.01	0.11	1.1×10^5	5.5×10^4

[a] The mean field calculation of G_0 is given for comparison. Δ characterizes the power law frequency dependence of G'' and ($G' - G_0'$) and not the critical values at the gel point.

With increasing φ at a fixed value of r (see Figure 7), the cross-link density of the system increases. This leads to formation of larger branched polymers until at a critical value, φ_c, the system percolates and a gel is formed. The value of φ_c increases with decreasing cross-link density and is approximately 0.12 for $r = 0.9$; see Figure 1. Again close to the gel point G' and G'' have a power law frequency dependence at low frequencies. We observed that the power law exponent at the gel point (Δ_c) increases with increasing φ: $\Delta_c = 0.25$, 0.31, 0.51, and 0.71 for $\varphi = 0.048$, 0.10, 0.40, and 0.90, respectively. Lusignan et al.[12] summarized experimental results for a number of systems and showed that Δ_c decreases if M_c/M_e increases. For $M_c/M_e < 2$, Δ_c is about 0.7 predicted for unentangled systems, while for $M_c/M_e \gg 1$, Δ_c is about 0.3. For the present system M_c/M_e is 13, 6, 1, and 0.2 for $\varphi = 0.048$, 0.10, 0.40, and 0.90, respectively.

For all gelled samples we find that at low frequencies G'' has a power law frequency dependence $G'' \propto \omega^{\Delta}$, although at $\varphi = 0.048$ it is not obvious and only reached at the lowest frequencies. The same power law frequency dependence is observed for $G' - G_0$, as was reported earlier for end-linked star PPO at different connectivity extents and with different molar masses.[13] One example of the subtraction is shown in Figure 7 for $\varphi = 0.249$. The subtraction allows us to determine an unambiguous value of G_0 even if the plateau is not clearly observed in the experiment. The values of Δ and G_0 are summarized in Table 1.

Discussion

The system we have investigated may be viewed as a melt of polydisperse linear chains that contain trifunctional units at random positions that cross-link the chains. The density of trifunctional units depends on φ while the density of free ends depends on r. Thus by increasing r at a given value of φ we increase the average molar mass of the linear chains, whereas by increasing φ at a given value of r we decrease M_c. The concentration of cross links that are elastically active, i.e., contribute to G_0, depends on both r and φ.

By use of mean field theory, one may calculate G_0 as a function of r and φ by assuming affine deformation; see Appendix. Note that the theoretical predictions are sensitive to the value of r and φ if they are close to the critical values. Close to the gel point the calculations are also sensitive to the exact reaction extent and the functionality. The theoretical values of G_0 are compared with the experimental results in Table 1. With one exception, the experimental results are within a factor of 2 of the theoretical predictions.

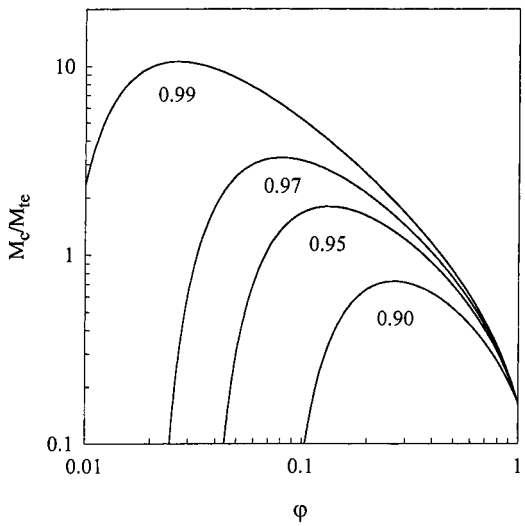

Figure 8. Ratio of the molar mass between cross-links and between trapped entanglements as a function of φ at different values of r indicated in the figure.

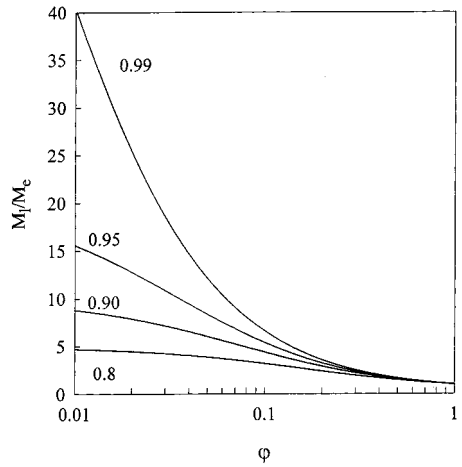

Figure 9. Ratio of the mean molar mass of linear chains and the entanglement molar mass as a function of φ at different values of r indicated in the figure.

When $M_c > M_e$ one needs to consider the presence of entanglements, because entanglements formed by segments that belong to the backbone of the network cannot relax and contribute to the gel modulus. The molar mass between trapped entanglements (M_{te}) is given by M_e and the elastic gel fraction (w_e): $M_{te} = M_e w_e^2$. The ratio M_c/M_{te} may be calculated by using mean field theory, see Appendix, and is shown as a function of φ at different values of r in Figure 8. It is clear that entanglements contribute significantly to G_0 only if r is very close to unity and φ is small. Rubinstein and Colby[14] used a scaling approach to calculate the contribution of entanglements to G_0 and came to the same conclusion.

However, even if the elastic network is not significantly entangled, entanglements do play an important role in the viscoelastic relaxation of the sol fraction and the dangling ends. The disentanglement process has been described in terms of the tube model.[15] In this model the lateral motion of a chain segment is assumed to be constrained to that of a tube formed by entanglements and covalent cross-links. An entanglement disappears as soon as a free end has reached the entanglement by diffusion through the tube. This process occurs either by reptation or by arm retraction, i.e., a chain end diffuses back through its own tube. For branched polymers and dangling ends, only the second process is possible. When an entanglement has disappeared, the effective molar mass between surviving entanglements has increased, i.e., the tube diameter has increased. This effect is called dynamic dilution because segments that have relaxed act as a solvent.

Recently the viscoelastic relaxation was investigated of randomly branched entangled polymers before the gel point.[9] For simple systems such as entangled stars the relaxation of shear modulus can be explicitly calculated. Unfortunately, such a calculation is unfeasible for polydisperse randomly branched polymers. For systems with $M_c \gg M_e$ one can use a scaling approach,[16] but as was shown in ref 9 the conditions where scaling applies are not accessible experimentally. Therefore we can only give a qualitative discussion of the results obtained in the present study.

Up to the gel point we need to consider only the sol. The first relaxation process after the conformational relaxation of chain segments between entanglements is the disentanglement of the linear chains of the sol. This relaxation process occurs via reptation and is characterized by a terminal relaxation time (τ_T) that increases as a power law with their number-average molar mass (M_l): $\tau_T \propto (M_l/M_e)^\alpha$. For most polymers $\alpha \approx 3.2$ has been observed.[17] In the present case τ_T is not well-defined because the linear sol chains are polydisperse. M_l can be calculated by mean field theory (see Appendix), and in Figure 9 we show M_l/M_e as a function of φ at different values of r. The dependence on r and φ of the experimentally observed relaxation time of the disentanglement of linear chains is consistent with the calculated variation of M_l/M_e. For large M_l the polydispersity index of the linear chains is 2; see Appendix. The amplitude of the relaxation of linear chains depends on their weight fraction, which may be calculated from mean field theory (see Appendix) and is shown as a function of φ in Figure 10 for $r = 0.9$ and $r = 0.99$. The weight fraction of linear sol chains decreases with increasing φ and is 0.25 at the gel point.

Once the linear chains have relaxed, the branched chains begin to relax. Close to the gel point the smaller branched polymers are still effectively entangled and relax by a process of arm retraction. The experimental results show that this gives rise to a power law frequency dependence of the shear modulus. However, due to the effect of dynamic dilution above a given size, the branched polymers are no longer effectively entangled; see ref 9. Their relaxation can be described in terms of a series of Rouse modes in same way as was done earlier for branched polymers based on unentangled precursors.[18] Therefore the exponent characterizes a smooth transition between the relaxation of the small entangled branched polymers and the larger effectively unentangled branched polymers. The terminal power law relaxation occurs at frequencies that are not accessible experimentally even for weakly entangled systems, because the relaxation time of arm retraction increases exponentially with the number of entanglements per arm.

Above the gel point we need to consider the contribution of the weight fraction of the sol (w_s), of the dangling ends (w_d), and of the elastic network (w_e), which may be calculated by using mean field theory; see Appendix. w_s and w_d are shown as a function of φ in Figure 10 for $r = 0.9$ and $r = 0.99$. With increasing φ, w_s decreases rapidly while w_d increases for $\varphi > \varphi_c$ up to a maximum,

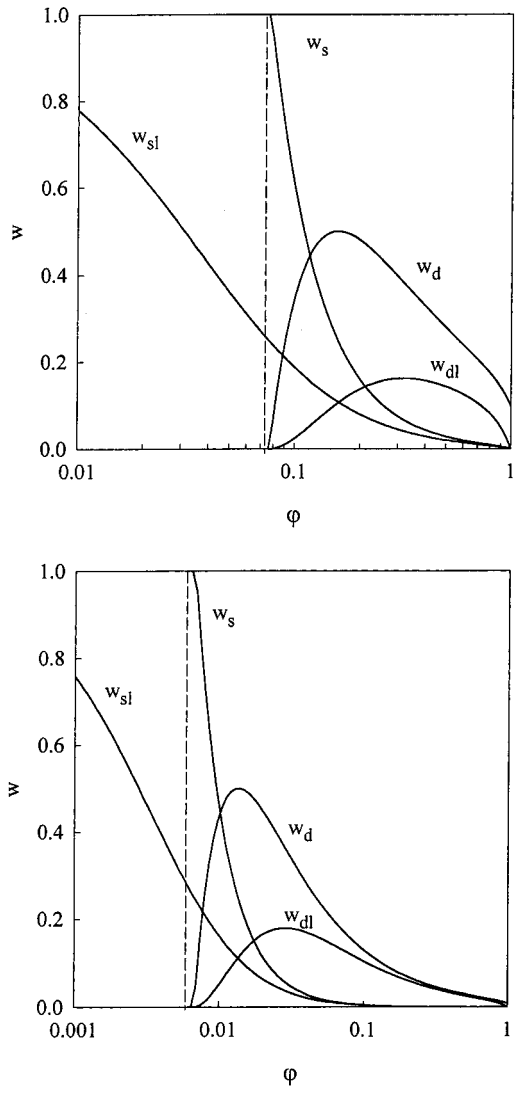

Figure 10. Dependence on φ of the fraction of the sol (w_s), the linear chains of the sol (w_{sl}), the dangling ends (w_d), and the linear dangling ends (w_{dl}) at $r = 0.9$ (top) and $r = 0.99$ (bottom). The dashed lines indicate the gel point.

after which it decreases again. $w_e = 1 - w_s - w_d$ and increases monotonically for $\varphi > \varphi_c$. The experimental results show that once the linear chains of the sol have relaxed, the combined relaxation of the branched sol chains and the dangling ends gives rise to a power law frequency dependence of G'' and $(G' - G_0)$. Just after the gel point the contribution of the sol dominates, but at larger φ the contribution of the dangling ends is most important.

Curro et al.[19] developed a theory to explain the power law frequency dependence of large weakly cross-linked but strongly entangled chains, i.e., with r close to unity and $\varphi \ll 1$. They assumed that the power law frequency dependence is caused by the relaxation of linear dangling ends. The size distribution of linear dangling ends and thus their mean length is the same as that of linear sol chains. They used mean field theory for the distribution of linear dangling ends and a theory given by Helfland and Pearson that was developed to describe the viscoelastic relaxation of star polymers.[20] Their theory predicts that for $\omega \ll \omega_R$ the shear modulus has a power law frequency dependence with an exponent that decreases linearly with decreasing cross-link density. More recently, McLeish and Milner[21] showed how the effect of dynamic dilution, which was ignored in ref 20, can be taken into account in the description of the viscoelastic relaxation of star polymers. This effect may be included in the calculation of the viscoelastic relaxation of dangling ends, and its effect is to modify the values of the power law exponent.

It should be remembered, however, that a power law frequency dependence is also observed in unentangled systems at and above the gel point. One such system was studied systematically as a function of the connectivity extent and showed a clear minimum in the exponent at a connectivity extent slightly larger than r_c.[18] As mentioned in the introduction, the power law frequency dependence of unentangled systems at the gel point with exponent $\Delta = \Delta_c$ may be understood in terms of the conformational relaxation of self-similar branched clusters of the sol that have a power law size distribution. After the gel point the relaxation of the branched structure between elastically active cross-links should be considered as well, which leads to a decrease of the power law exponent Δ with increasing r. At larger connectivity extents the sol fraction becomes negligible while the average distance between elastically active cross links decreases and the gel modulus increases. At frequencies where the gel modulus dominates G', G'' still shows a power law frequency dependence that is caused by the relaxation of dangling ends on length scales larger that the average distance between cross-links. With increasing r the distribution of dangling ends decreases more sharply, resulting in an increase of Δ.

The crucial assumption in the theory of Curro et al. is that the viscoelastic relaxation for $\omega < \omega_R$ is dominated by that of linear dangling ends. The fraction of linear dangling ends may be calculated from mean field theory and is plotted as a function of φ in Figure 10 for $r = 0.9$ and $r = 0.99$. Figure 10 shows that the assumption that the contribution of branched dangling ends and sol chains may be ignored is reasonable only for r very close to unity and φ not close to φ_c. These conditions are difficult to achieve and in practice the contribution of branched chains may not be neglected. Nevertheless, one may understand qualitatively the increase of the exponent with increasing φ, because the larger is φ the sharper is the decrease of the number of sol chains and dangling ends with increasing molar mass. For the same reason, the exponent increases when r approaches unity.

The relaxation of the elastic network is often assumed to be limited to the normal modes relaxation of chain segments between covalent cross-links or trapped entanglements at high frequencies that cross over to a purely elastic response, i.e., with $G'' \propto \omega$, at low frequencies. This means that if $r \to 1$, and thus $w_e \to 1$, the exponent Δ should approach 1. Indeed for larger φ, Δ increases with increasing r and approaches unity; see ref 9. But these systems are no longer entangled.

A result that cannot be explained in terms of relaxation by arm retraction of dangling ends is the distinct entanglement plateau modulus for G' and the corresponding weak maximum or shoulder in G''. These features are observed for all systems as long as $M_l/M_e > 1$, even if the sol fraction is small and cannot be attributed to disentanglement of linear sol chains. For instance, gels at $\varphi = 0.048$, with $M_l/M_e > 10$, show a significant decay of G' between $G(\omega_R)$ and G_0 even for the system closest to $r = 1$; see Figure 6. Figure 10

shows that for r very close to 1 and φ not too close to φ_c, i.e., the conditions where the theory by Curro et al. may be applied, w_d and w_s are much smaller than w_e, implying that $[G'(\omega_R) - G_0] \ll G_0$. In addition, for these samples we do not observe a power law decay of G'' except perhaps over a limited range of the lowest frequencies. We tentatively attribute the maximum in G'' and the distinct plateau modulus to the relaxation of trapped entanglements. Notice that in the experimentally accessible frequency range many of the entanglements formed by dangling ends cannot relax by a process of arm retraction and should be considered as trapped. As mentioned above, it was found from computer simulations that about 50% of the trapped entanglements in the elastic network relax on the time scale probed in the simulations. This would explain a decay of G' by a factor of 2. Apparently, in the present system a larger fraction of entanglements decays. Notice, however, that G' decays very slowly, and in ref 7 G_0 was estimated from G' at frequencies not very much lower than ω_R.

The question is by what process trapped entanglements relax. From the shape of the curves in Figure 6 it appears that at least the initial relaxation of trapped entanglements occurs by the same process as that of linear chains in the melt. We note that the mean length of linear chain segments between covalent cross-links is the same as that of linear sol chains and is given in Figure 9. We have no answer to this question, but the experimental results point to a reptation process of linear chain segments between covalent cross-links.

Conclusions

The combined relaxation of entangled sol and dangling ends gives rise to a low-frequency power law frequency dependence of G'' and $G' - G_0$ at and above the gel point. Small values of the exponent Δ are observed (≤ 0.3) for systems with low cross-link density. The observed power law frequency dependence at and above the gel point represents a crossover to the terminal relaxation, which is not influenced by entanglements between branching points. However, even a small number of entanglements between branching points render experimental observation of this terminal power law frequency dependence impossible.

Mean field calculations show that the fraction of entanglements trapped in the elastic network is only significant if the system has a very low cross-link density and a connectivity extent close to unity.

For all weakly cross-linked gels we observed a distinct relaxation process that corresponds to the reptation of linear entangled chains. This relaxation process was observed even for systems where the sol fraction is small.

Appendix

Here we summarize the mean field results that we use for the interpretation of the experimental results. Details for the derivations can be found in refs 22−24.

The molar fractions of HMDI, PPO diol, and PPO triol are related to the connectivity extent r and the fraction q of hydroxyl groups belonging to PPO triol as follows:

$$n_{B2} = \frac{3(1-q)}{[3(1+r)-q]}$$

$$n_{B3} = \frac{2q}{[3(1+r)-q]}$$

$$n_A = \frac{3r}{[3(1+r)-q]}$$

where $q = 3\varphi/(2+\varphi)$ with φ, the cross-link density.

The number-average (M_{n0}) and weight-average (M_{w0}) molar masses of the starting material are

$$M_{n0} = n_A M_A + n_{B2} M_{B2} + n_{B3} M_{B3}$$

$$M_{w0} = \frac{n_A M_A^2 + n_{B2} M_{B2}^2 + n_{B3} M_{B3}^2}{M_{n0}}$$

where M_A, M_{B2}, and M_{B3} are the molar masses of HMDI, PPO diol, and PPO triol, respectively.

The fraction of reacted isocyanate groups is p_A and that of reacted hydroxyl groups is $p_B = r p_A$. The critical reaction extent at the gel point is

$$p_{A,c} = \left[\frac{1}{r(1-q)}\right]^{1/2} \quad \text{(A1)}$$

In the following we will assume complete reaction, i.e., p_A or $p_B = 1$, so that the sol−gel diagram is given by the following relations:

$$r_{c,min} = \frac{1}{1-q} \; (p_A = 1)$$

and

$$r_{c,max} = 1 - q \; (p_B = 1) \quad \text{(A2)}$$

The composition of the polyurethane formed by end-linking can be characterized by the number of PPO diol (i), PPO triol (j), and HMDI (k) molecules. If we assume again complete reaction, then $k = i + j - 1$ for $r < 1$ and $p_B = r$. In this particular case the molar fraction of macromolecules with a particular composition (i, j) is given by

$$n(i,j) = \frac{6(i+2j)!}{[3(1-r)-q]i!j!(j+2)!} \times q^j(1-q)^i r^{i+j-1}(1-r)^{j+2} \quad \text{(A3)}$$

The weight fraction is given by

$$w(i,j) = n(i,j)\frac{[3(1-r)-q]}{[3(1+r)-q]} \times \frac{[iM_{B2} + jM_{B3} + (i+j-1)M_A]}{M_{n0}} \quad \text{(A4)}$$

To calculate the statistical properties of the gels we use the probabilities that an isocyanate group (π_A) or a hydroxyl group (π_B) selected at random will lead to finite chains:

$$\pi_A = (1 - p_A) + p_A q$$

$$\pi_B^2 + p_A(1-q)\pi_B$$

where $\pi_B = (1 - p_B) + p_B \pi_A$.

Table 2.

xy	A_{xy}	M_{xy}(i)	$M_{xy} = \sum_{i=1} M_{xy}(i)X^{i-1}$
sl	$(1-r)^2$	$iM_{B2} + (i-1)M_A$	$\frac{M_{B2}+M_A}{(1-X)^2} - \frac{M_A}{(1-X)}$
se	$[qr(1-\pi_B)^2]^2$	$iM_{B2} + {}^2/_3M_{B3} + (i+1)M_A$	$\frac{M_{B2}+M_A}{(1-X)^2} + \frac{M_A}{(1-X)} + \frac{2M_{B3}}{3(1-X)}$
sd	$2(1-r)qr\,(1-\pi_B)^2$	$iM_{B2} + {}^1/_3M_{B3} + iM_A$	$\frac{M_{B2}+M_A}{(1-X)^2} + \frac{M_A}{(1-X)} + \frac{M_{B3}}{3(1-X)}$

It follows that at complete reaction

$$\pi_A = 1 \text{ and } \pi_B = 1 \quad \text{for } r < r_{c,min} \text{ and } r > r_{c,max}$$

$$\pi_A = \frac{(1-r)(1-rq)}{r^2 q}; \quad \pi_B = \frac{(1-r)}{rq} \text{ for } 1 > r > r_{c,min}$$

$$\pi_B = \pi_A = \frac{(r-1)}{q} \quad \text{for } 1 < r < r_{c,max}$$

The weight fractions of the sol (w_s), dangling chains (w_d), and elastic chains (w_e) are given by

$$w_S = \frac{n_A \pi_A{}^2 M_A + n_{B2} \pi_B{}^2 M_{B2} + n_{B3} \pi_B{}^3 M_{B3}}{M_{n0}}$$

$$w_d = [2n_A(1-\pi_A)\pi_A M_A + 2n_{B2}(1-\pi_B)\pi_B M_{B2} + n_{B3}\pi_B(1-\pi_B)[3\pi_B + (1-\pi_B)]M_{B3}]/M_{n0} \quad \text{(A5)}$$

$$w_e = 1 - w_S - w_d$$

and w_{gel} is equal to $1 - w_S$. The number of elastically active network chains per unit of mass is

$$\nu = \frac{3(1-\pi_B)^3 N_a}{M_{n0}[3(1+r) - q]} \quad \text{(A6)}$$

where N_a is Avogadro's number.The probability $n_l(i)$ of forming a linear chain or chain fragment, i.e., consisting solely of PPO diol and HMDI, with a number *i* of PPO diols is independent of the position of the chain fragments in larger structures and is given by

$$n_l(i) = n_{B2} X^{i-1} \quad \text{(A7)}$$

with $X = r(1-q)$.

The number- and weight-average degrees of polymerization of these linear chain fragments and their polydispersity index are given by

$$DP_{ln} = \frac{\sum in(i)}{\sum n(i)} = \frac{1}{(1-X)}$$

$$DP_{lw} = \frac{\sum i^2 n(i)}{\sum in(i)} = \frac{(1+X)}{(1-X)}$$

$$I = \frac{DP_{lw}}{DP_{ln}} = 1 + X \quad \text{(A8)}$$

The weight fractions (w_{xy}) of linear sol chains (w_{sl}), linear dangling chains (w_{dl}), and linear elastic chains (w_{el}) are determined by the probability that the linear chain fragment has, respectively, two free ends; one free end and one end connected to the elastic network; and two ends connected to the elastic network. Notice that these probabilities are not exhaustive. The weight fractions are given by

$$w_{xy} = \frac{n_{B2} A_{xy} M_{xy}}{M_{n0}} \quad \text{(A9)}$$

where A_{xy} and M_{xy} are given in Table 2.

$M_{xy}(i)$ is the molar mass of a linear chain fragment composed of *i* diol and M_{xy} is the number-average molar mass of linear chain fragments of type *xy*.

The first term of each sum composing M_{xy} represents the major contribution to M_{xy}, so that the number-average molar mass of linear chain fragments (M_l) is approximately independent of their position and is given by

$$M_l = \frac{M_{B2} + M_A}{(1-X)^2} \quad \text{(A10)}$$

The number-average molar mass of between two branching points, M_c, is thus equal to M_l.

References and Notes

(1) Flory, P. J. *Principles of Polymer Chemistry*; Cornell University Press: Ithaca, NY, 1953.

(2) Stockmayer, W. H. *J. Chem. Phys.* **1943**, *11*, 45; *J. Chem. Phys.* **1944**, *12*, 125.

(3) Stauffer, D.; Aharony, A. *Percolation theory*, 2nd ed.; Taylor & Francis: London, 1992.

(4) Martin, J. E.; Adolf, D. *Annu. Rev. Phys. Chem.* **1991**, *42*, 311.

(5) Rubinstein, M.; Colby, R. H.; Gillmor, J. R. In *Space-Time Organization in Macromolecular Fluids*; Tanaka, F., Doi, M., Ohta, T., Eds.; Springer-Verlag: Berlin, 1989.

(6) Eg, M. J.; Erman, B. *Rubberlike Elasticity*; John Wiley & Sons: New York, 1988.

(7) Duering, E. R.; Kremer, K.; Grest, G. S. *J. Chem. Phys.* **1994**, *110*, 8169.

(8) Patel, S. K.; Malone, S.; Cohen, C.; Gillmor, J. R.; Colby, R. *Macromolecules* **1992**, *25*, 5241.

(9) Nicol, E.; Nicolai, T.; Durand, D. *Macromolecules* **2001**, *34*, 5205.

(10) Prochazka, F.; Nicolai, T.; Durand, D. *Macromolecules* **2000**, *33*, 1703.

(11) Nicolai, T.; Floudas, G. *Macromolecules* **1998**, *31*, 2578.

(12) Lusignan, C. P.; Mourey, T. H.; Wilson, J. C.; Colby, R. H. *Phys. Rev. E* **1999**, *60*, 5657.
(13) Nicolai, T.; Prochazka, F.; Durand, D. *J. Rheol.* **1999**, *43*, 1511.
(14) Rubinstein, M.; Colby, R. H. *Macromolecules* **1994**, *27*, 3184.
(15) Wanatabe, H. *Prog. Polym. Sci.* **1999**, *24*, 1253−1403.
(16) Rubinstein, M.; Zurek, S.; McLeish, T. C. B.; Ball, R. C. *J. Phys. France* **1990**, *51*, 757.
(17) Ferry J. D. *Viscoelastic Properties of Polymers*, 2nd ed; Wiley: New York, 1970.
(18) Nicolai, T.; Randrianantoandro, H.; Prochazka, F.; Durand, D. *Macromolecules* **1997**, *30*, 5897.
(19) Curro, J. G.; Pearson, D. S.; Helfand, E. *Macromolecules* **1985**, *18*, 1157.
(20) Helfland, E.; Pearson, D. S. *J. Chem. Phys.* **1983**, *79*, 2054.
(21) McLeish, T. C. B.; Milner, S. T. *Adv. Polym. Sci.* **1999**, *143*, 195.
(22) Macosko, C. W.; Miller, D. R. *Macromolecules* **1976**, *9*, 199.
(23) Durand, D.; Bruneau, C. M. *Macromolecules* **1979**, *12*, 1216.
(24) Durand, D.; Bruneau, C. M. *Makromol. Chem.* **1982**, *183*, 1021.

MA011412A